Electronic Supplementary Material (ESI) for Journal of Materials Chemistry A.
This journal is © The Royal Society of Chemistry 2021

Supporting Information

Real-time monitoring of electrochemical carbon corrosion in alkaline media

Sang Gu Ji[a], Haesol Kim[a], Woong Hee Lee[b], Hyung-Suk Oh[b] and Chang Hyuck Choi*[a]

[a]*School of Materials Science and Engineering, Gwangju Institute of Science and Technology, Gwangju 61005, Republic of Korea.*

[b]*Clean Energy Research Center, Korea Institute of Science and Technology (KIST), Hwarang-ro 14-gil 5, Seongbuk-gu, Seoul, 02792, Republic of Korea.*

**Corresponding author: chchoi@gist.ac.kr*

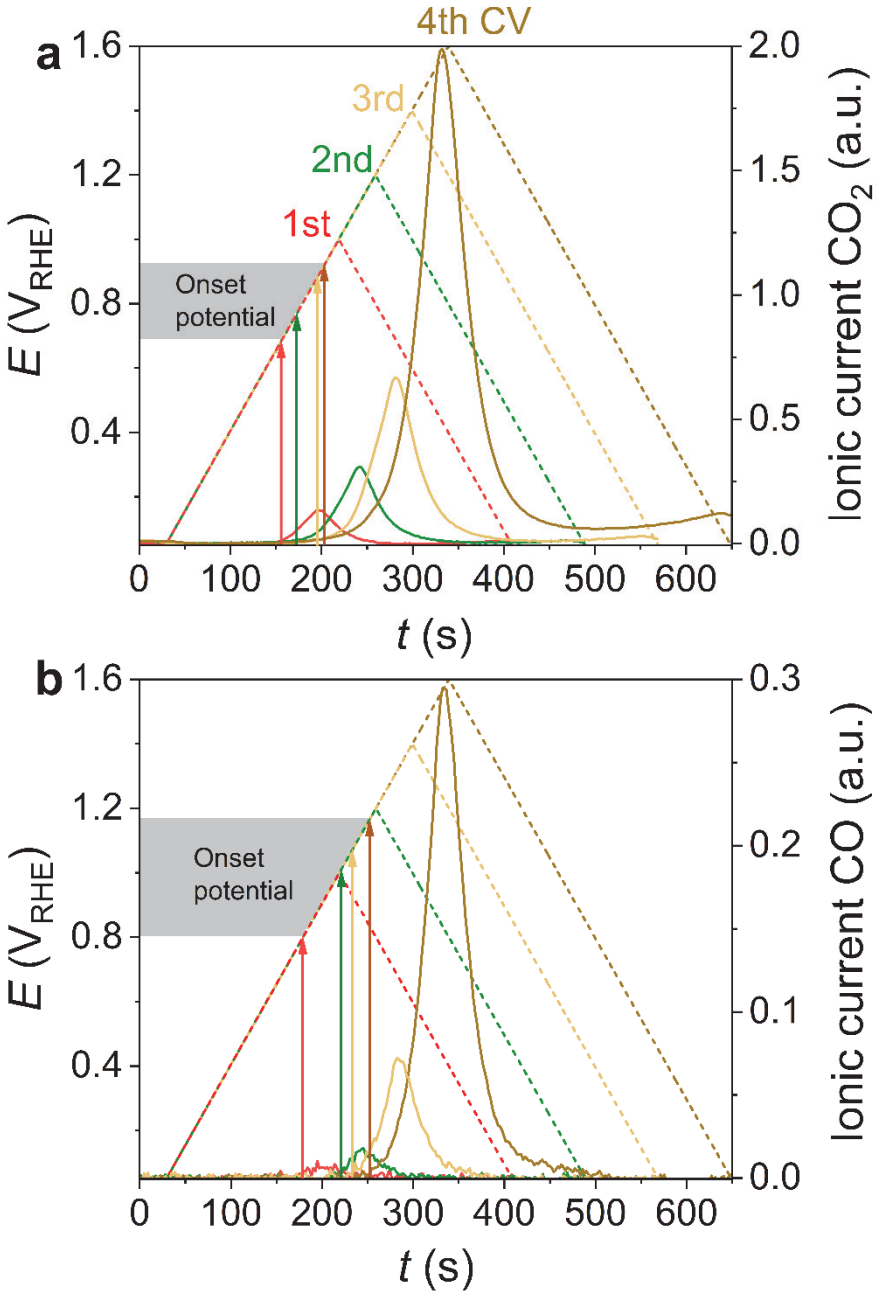

Figure S1. Magnified ionic current signals of (a) CO_2 and (b) CO for Vulcan in an Ar-saturated 0.1 M $HClO_4$ electrolyte during the CV protocol. All potential profiles of the CV protocol (dotted line, left y-axis) and ionic current signals (solid line, right y-axis) are overlaid for better comparison. Arrows indicate the onset potentials of the carbon corrosion monitored by the DEMS signals.

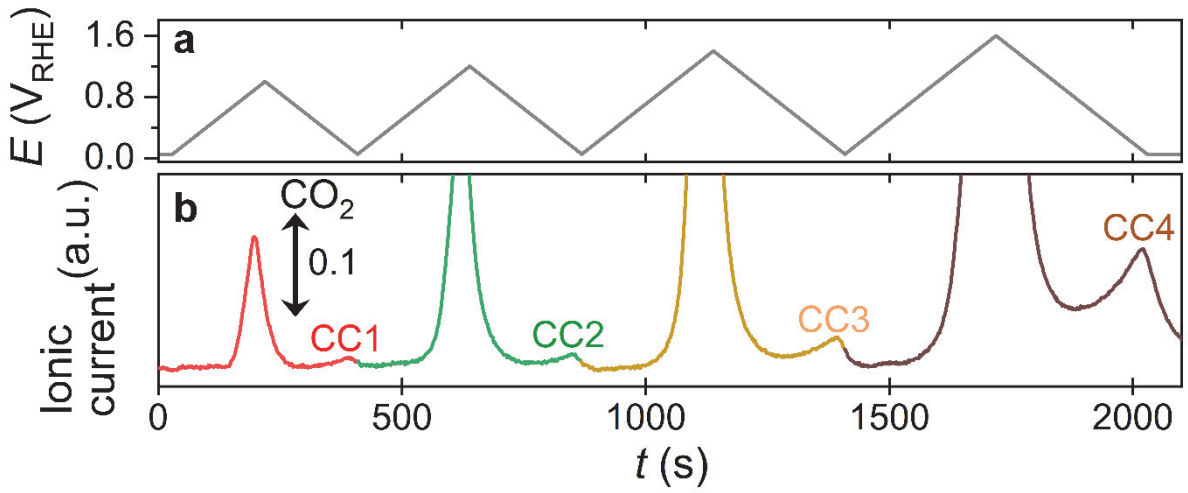

Figure S2. Magnified ionic current signal of CO_2 for Vulcan in an Ar-saturated 0.1 M $HClO_4$ electrolyte during the CV protocol: (a) potential protocol and (b) ionic current signal of CO_2. Cathodic corrosions are denoted as CCx (x = 1–4) according to the CV sequence.

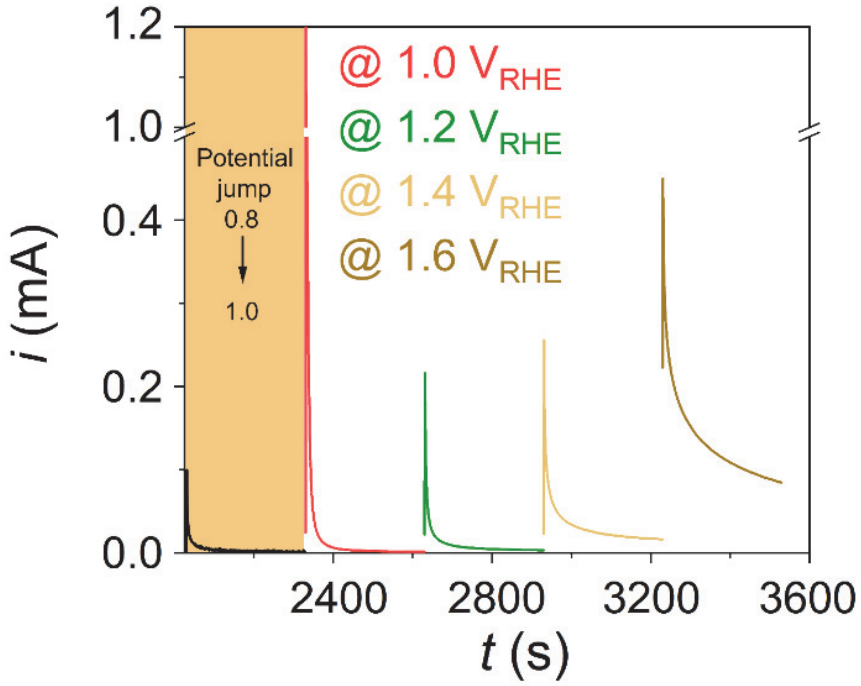

Figure S3. The current-time responses measured during the CA protocol. Potential jumped from 0.05 to 1.0 V_{RHE} (red line), from 1.0 to 1.2 V_{RHE} (green line), from 1.2 to 1.4 V_{RHE} (yellow line), and then from 1.4 to 1.6 V_{RHE} (brown line) just before each CA measurement. Due to the significant potential changes in the first CA, from 0.05 to 1.0 V_{RHE} (red line), and the consecutive significant current contributions from non-Faradaic current, the current-time response during the CA measurement at 1.0 V_{RHE} was additionally measured with an initial potential-jump from 0.8 to 1.0 V_{RHE} and shown for comparison (black line, marked in the orange area).

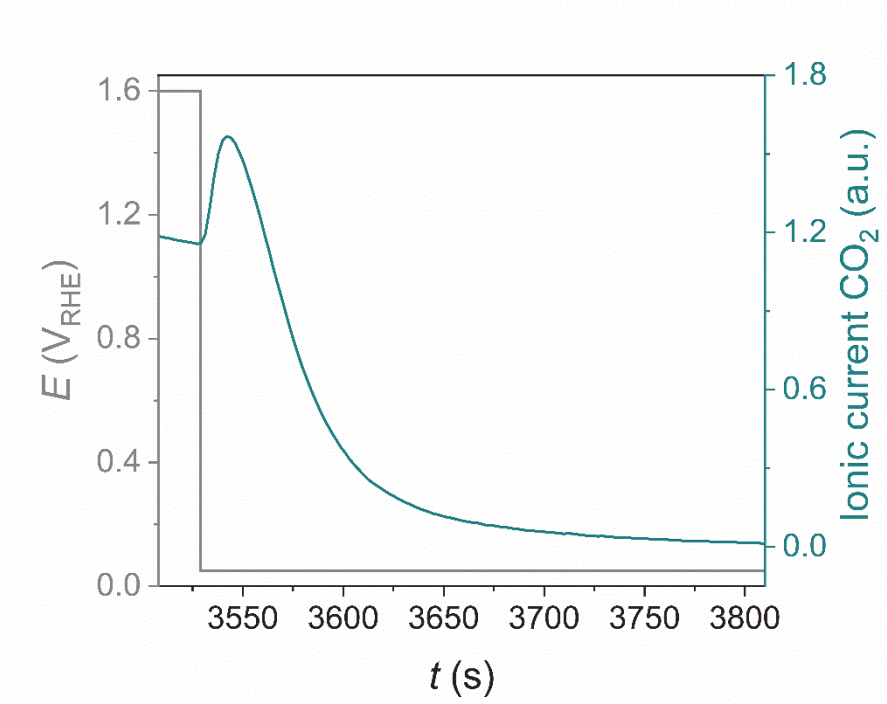

Figure S4. Magnified ionic current signal of CO_2 for Vulcan in an Ar-saturated 0.1 M $HClO_4$ electrolyte at the end of the CA protocol, potential-jump from 1.6 to 0.05 V_{RHE}.

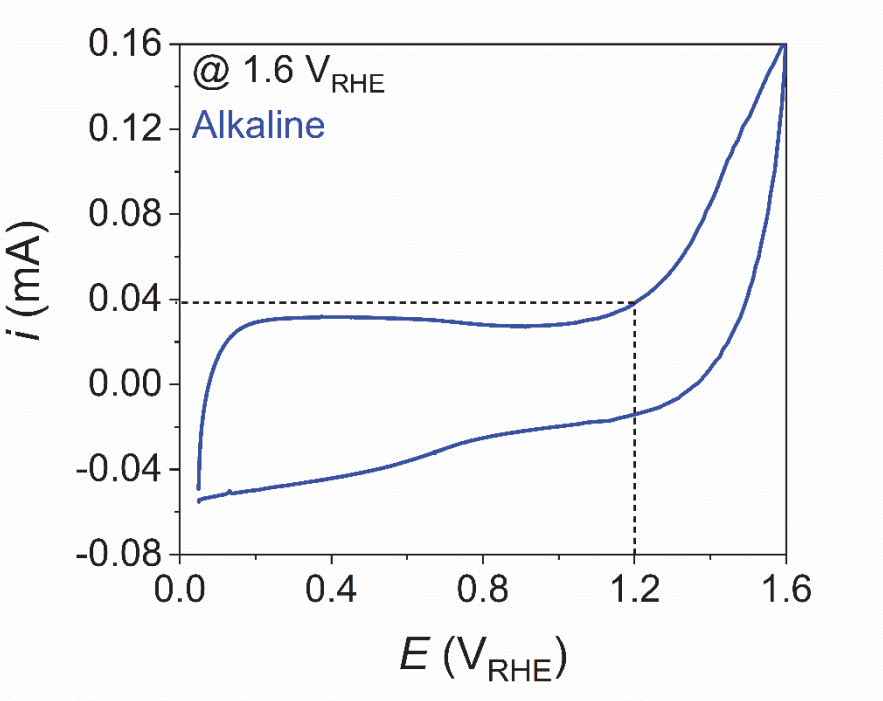

Figure S5. A CV response of Vulcan measured in a potential range of 0.05–1.6 V_{RHE} at a scan rate of 5 mV s^{-1} in an Ar-saturated 0.1 M KOH electrolyte. Oxidation current can be identified at potential above 1.2 V_{RHE}, indicated by the dotted line.

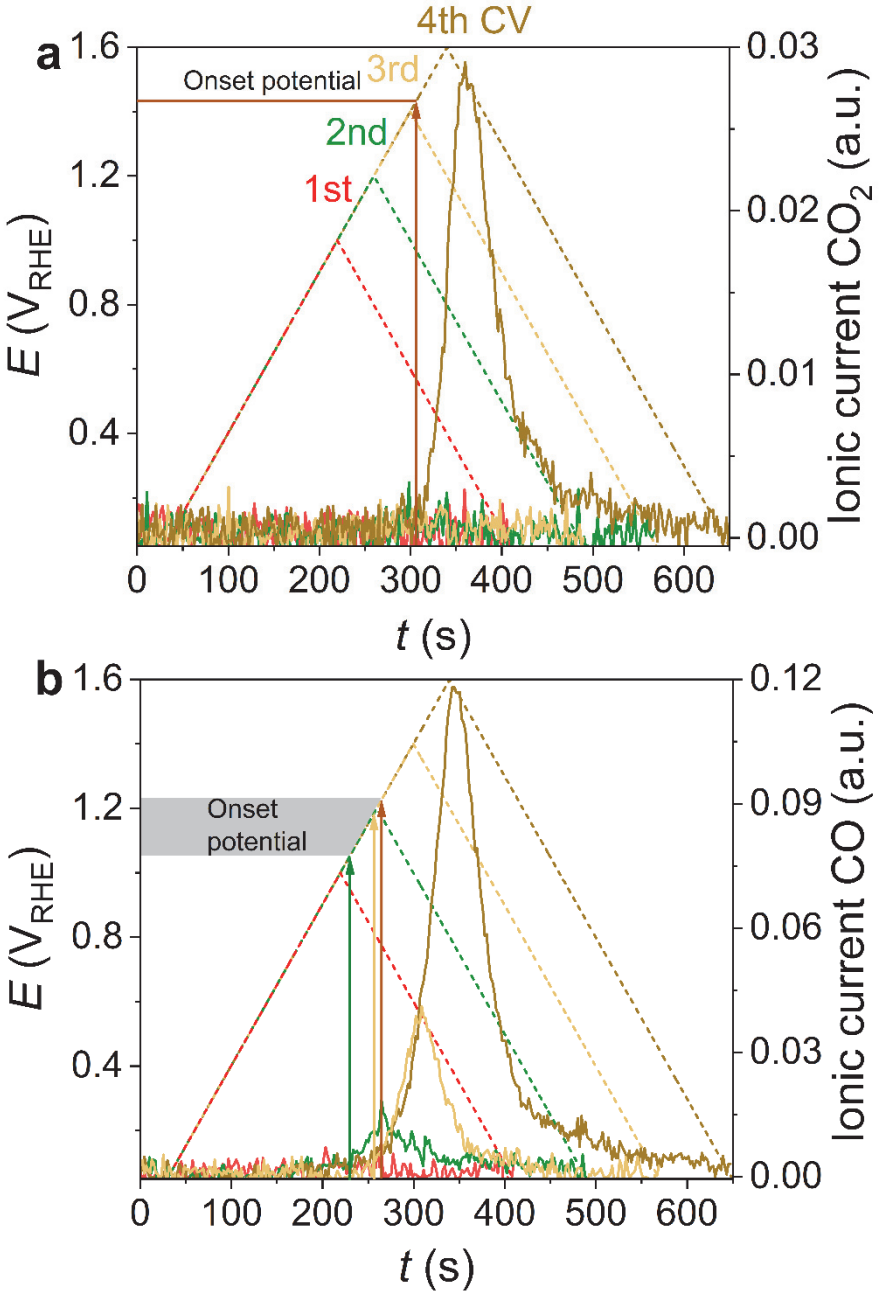

Figure S6. Magnified ionic current signals of (a) CO_2 and (b) CO for Vulcan in an Ar-saturated 0.1 M KOH electrolyte during the CV protocol. All potential profiles of the CV protocol (dotted line, left y-axis) and ionic current signals (solid line, right y-axis) are overlaid for better comparison. Arrows indicate the onset potentials of the carbon corrosion monitored by the DEMS signals.

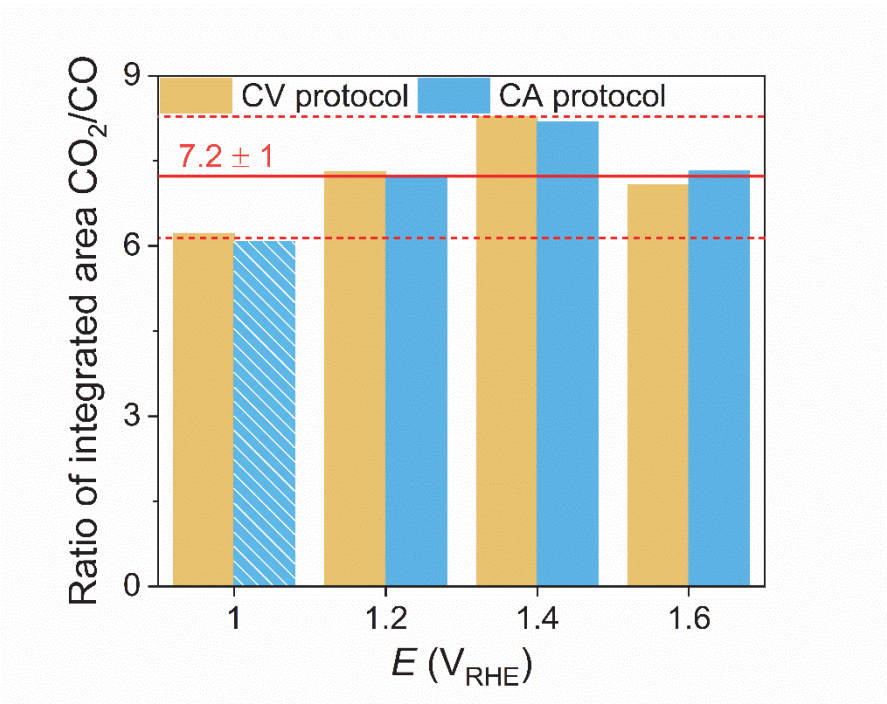

Figure S7. Integrated area ratio between CO_2 and CO DEMS signals monitored with Vulcan during the CV (yellow bar) and CA (blue bar) protocols in an Ar-saturated 0.1 M $HClO_4$ electrolyte. For the CA protocol at 1 V_{RHE} (highlighted with white lines), the CO_2 and CO DEMS signals were gathered separately with an initial potential-jump from 0.8 to 1.0 V_{RHE} to avoid any artifacts induced by the large potential-jump from 0.05 to 1.0 V_{RHE} just before the CA protocol in the original potential program. The ratios are almost similar as *ca.* 7.2 with a deviation of ±1.

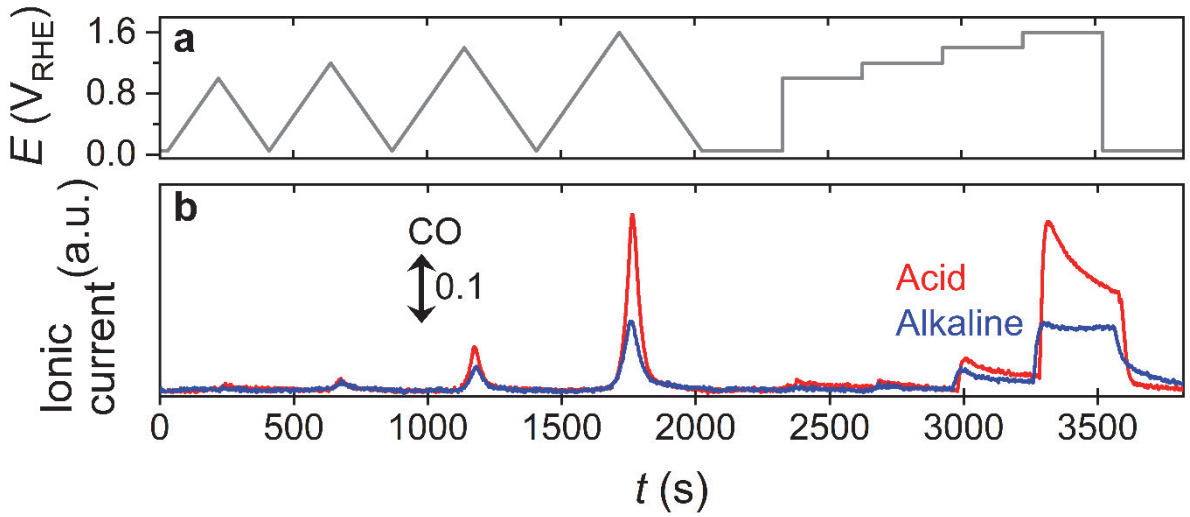

Figure S8. Comparison of the ionic current signals of CO for Vulcan measured in an Ar-saturated 0.1 M $HClO_4$ and KOH electrolytes: (a) potential protocol and (b) ionic current signal of CO.

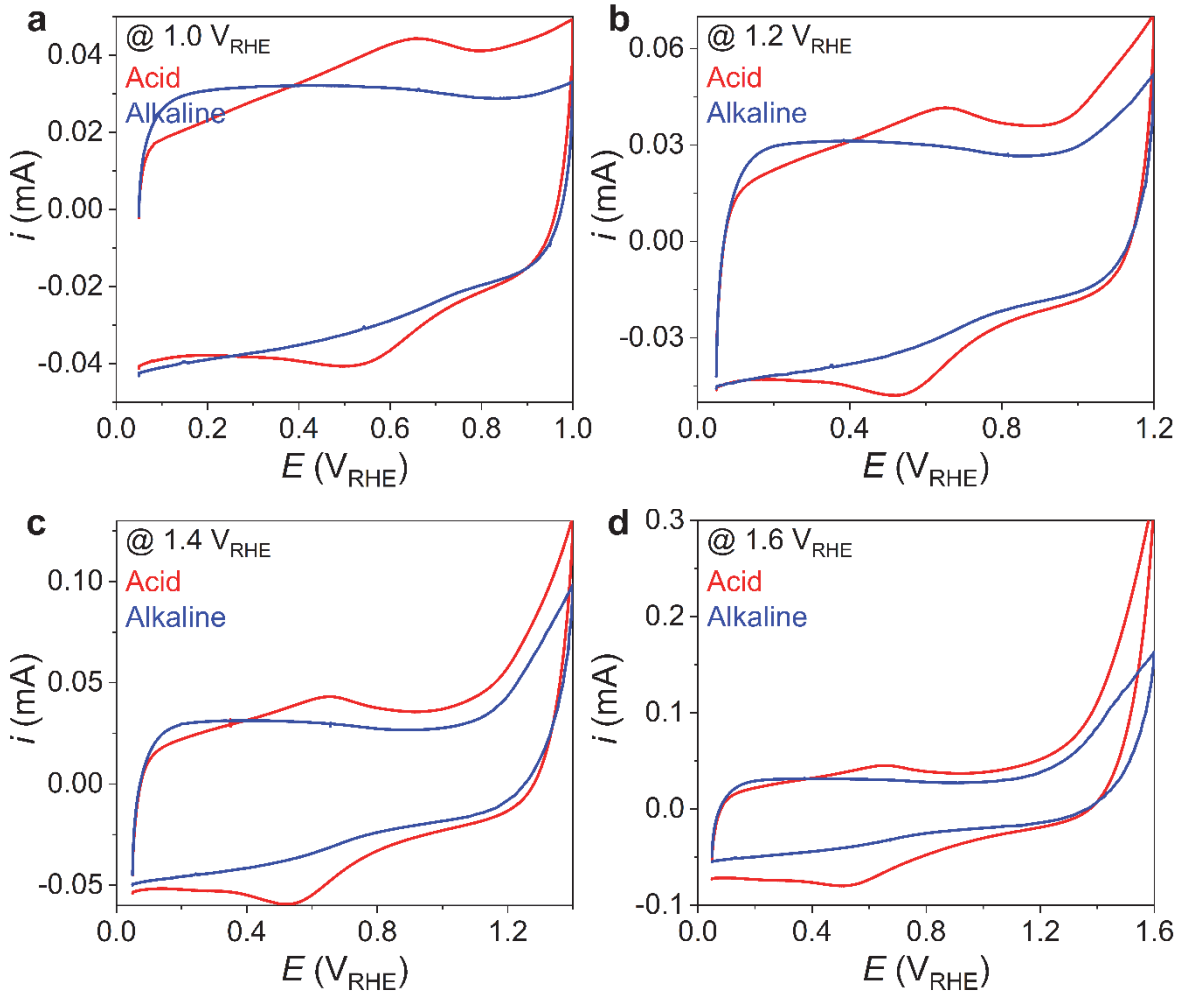

Figure S9. CV response of Vulcan in an Ar-saturated 0.1 M $HClO_4$ and KOH electrolytes with a scan rate of 5 mV s^{-1}. Potential range for the measurement was from 0.05 to (a) 1.0, (b) 1.2, (c) 1.4, and (d) 1.6 V_{RHE}.

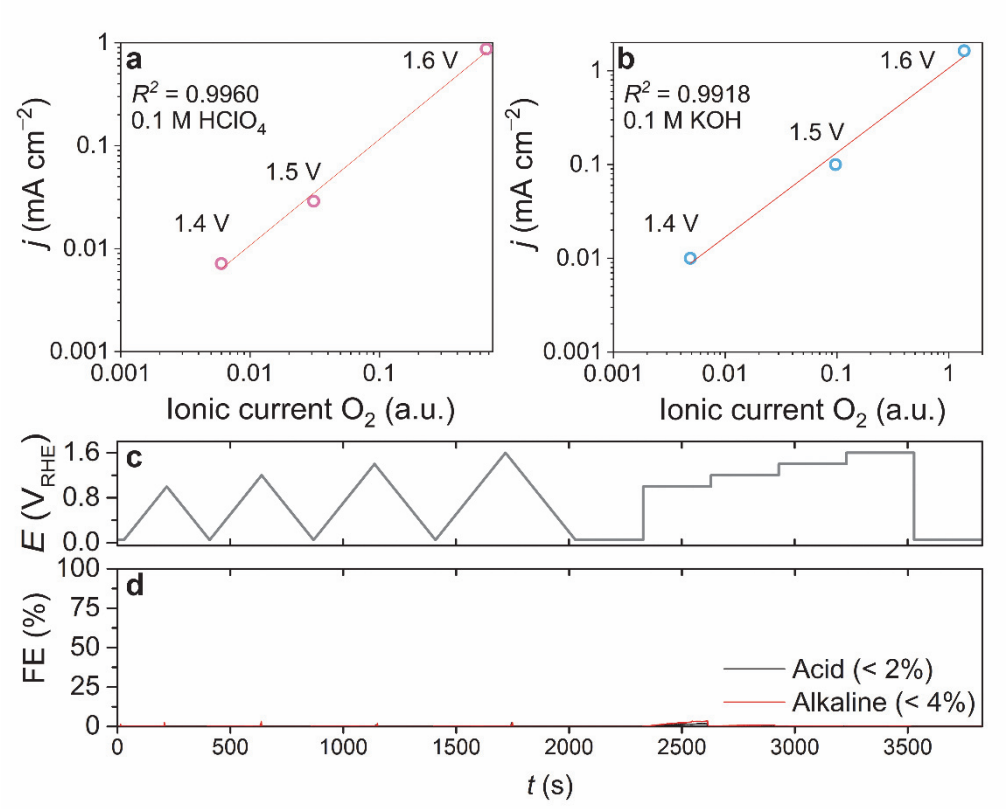

Figure S10. Online DEMS calibration curves for O_2 (m/z = 32) obtained with an IrO_2 catalyst in (a) 0.1 M $HClO_4$ and (b) 0.1 M KOH electrolytes. (c) The potential program consisting of four CVs with different UPLs (1.0, 1.2, 1.4, and 1.6 V_{RHE}) and four CAs at 1.0–1.6 V_{RHE}. (d) The Faradaic efficiencies of O_2 during the carbon corrosion measurement of Vulcan in both electrolyte conditions.

Note: The competitive reactions between carbon oxidation and oxygen evolution can lead to non-negligible errors in data interpretations. Hence, we attempted to quantitatively analyze the Faradaic efficiency toward oxygen evolution using an IrO_2 catalyst. Since no carbon substance is present in the catalyst, we can reasonably assume that the Faradaic current only originates from the oxygen evolution, and not from other side reactions such as carbon corrosion. The correlations between the Faradaic current density and the ionic current signal of O_2 at m/z = 32 in acidic and alkaline electrolytes revealed very linear relationships with R^2 values of *ca.* 0.9960 and 0.9918, respectively (Figure S10a and b). Using these calibration curves, the Faradaic efficiency of O_2 evolved during the carbon corrosion of Vulcan was calculated. The results revealed that the Faradaic efficiencies of O_2 were as low as <2 and 4% in acidic and alkaline electrolytes during the overall DEMS protocol (Figure S10c and d), respectively, confirming that the oxidation currents of Vulcan are mainly attributed to carbon corrosion.

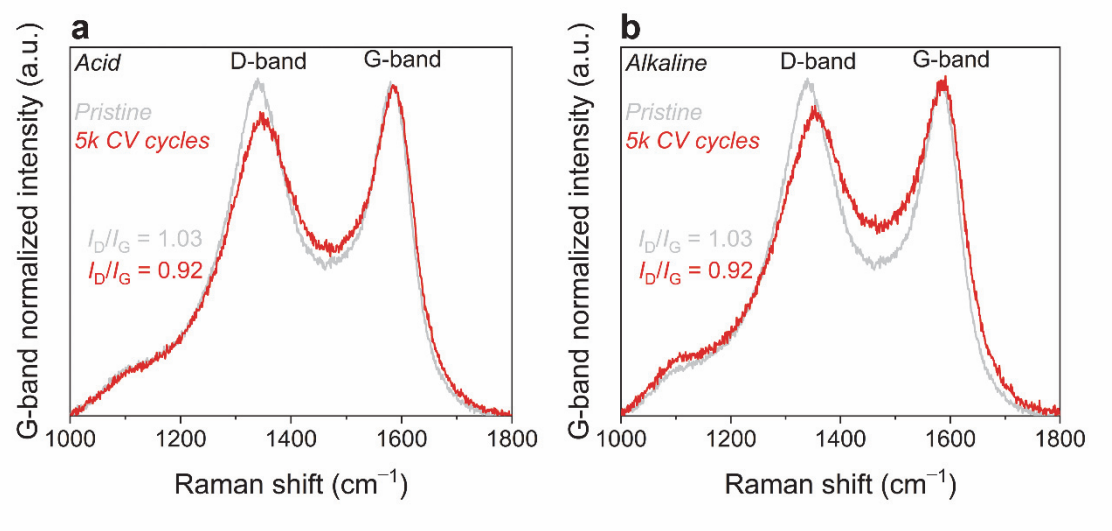

Figure S11. Raman spectra of Vulcan before and after carbon corrosion in (a) 0.1 M $HClO_4$ and (b) 0.1 M KOH electrolytes. The electrochemical treatment was carried out by 5000 CV cycles from 1.2 to 1.6 V_{RHE} at 50 °C to accelerate the carbon corrosion.

Note: To investigate the structural characteristics before and after carbon corrosion, Raman spectra of Vulcan were measured after electrochemical treatment. The electrochemical treatment was progressed by 5000 CV cycles (from 1.2 to 1.6 V_{RHE}, 200 mV s^{-1}) at 50 °C to accelerate the carbon corrosion. The Raman spectra, normalized to the G-band intensity, revealed a decrease in the ratio of D- and G-band intensities (I_D/I_G, a descriptor of carbon disorder) from *ca*. 1.03 to 0.92. These results thus indicate the preferential oxidation of the disordered domains of carbon in both acidic and alkaline electrolytes.

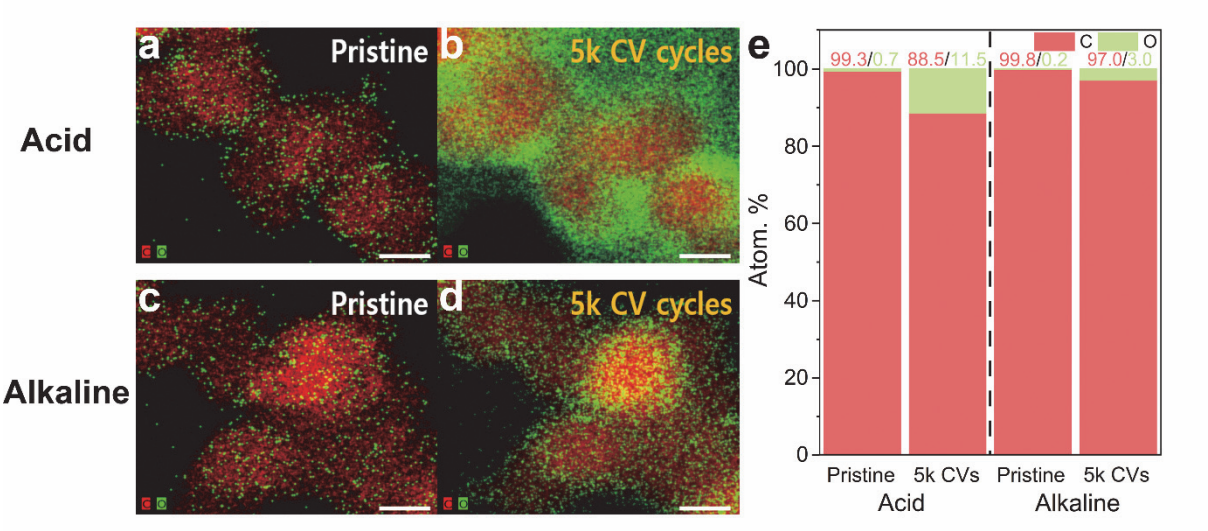

Figure S12. IL-EDX results of Vulcan before and after carbon corrosion in (a and b) 0.1 M $HClO_4$ and (c and d) 0.1 M KOH electrolytes (scale bar = 20 nm). The electrochemical treatment was carried out by 5000 CV cycles from 1.2 to 1.6 V_{RHE} at 50 °C to accelerate the carbon corrosion. (e) Carbon and oxygen contents before and after the treatment.

Note: In addition to the Raman spectroscopy study (Figure S11), the structural characteristics before and after carbon corrosion were investigated by IL-EDX measurements. The electrochemical treatment was progressed by 5000 CV cycles (from 1.2 to 1.6 V_{RHE}, 200 mV s^{-1}) at 50 °C to accelerate the carbon corrosion. The results showed that carbon surface was significantly passivated by oxygen after the electrochemical treatment (Figure S12a–d; red and green for carbon and oxygen, respectively). After the treatment, relatively stronger oxygen signals in the acidic electrolyte compared to the alkaline electrolyte indicates more pronounced carbon corrosion in the former condition. The IL-EDX profiles identified an increase in oxygen content from *ca*. 0.7 to 11.5 at% after carbon corrosion in the acid electrolyte (Figure S12e), which was greater than that in the alkaline electrolyte (from *ca*. 0.2 to 3.0 at%).

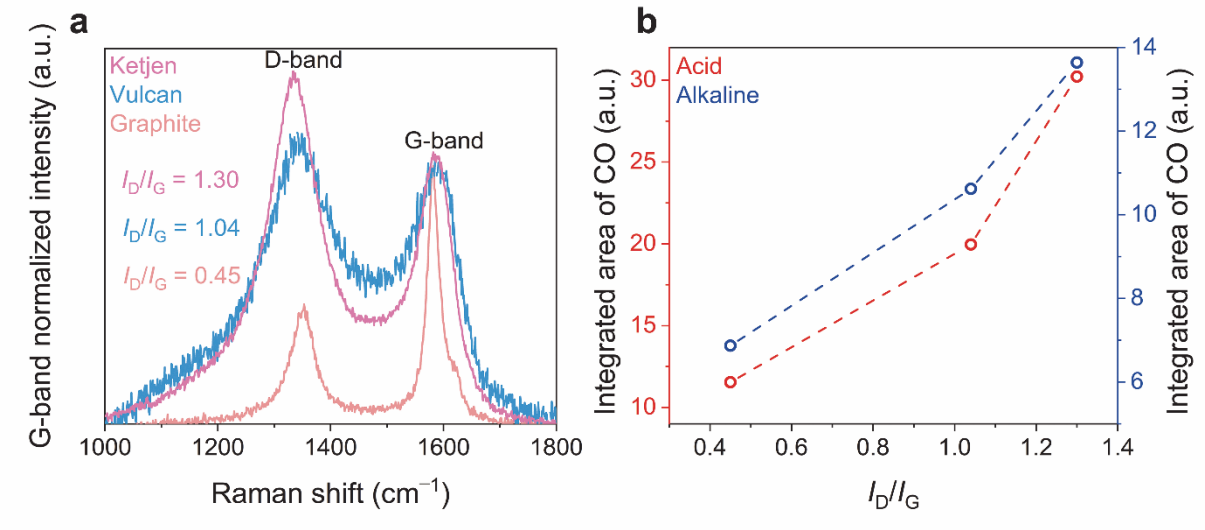

Figure S13. (a) Raman spectra of different carbon substrates. (b) Correlation between the I_D/I_G value and the integrated area of CO mass signal in acidic and alkaline electrolytes.

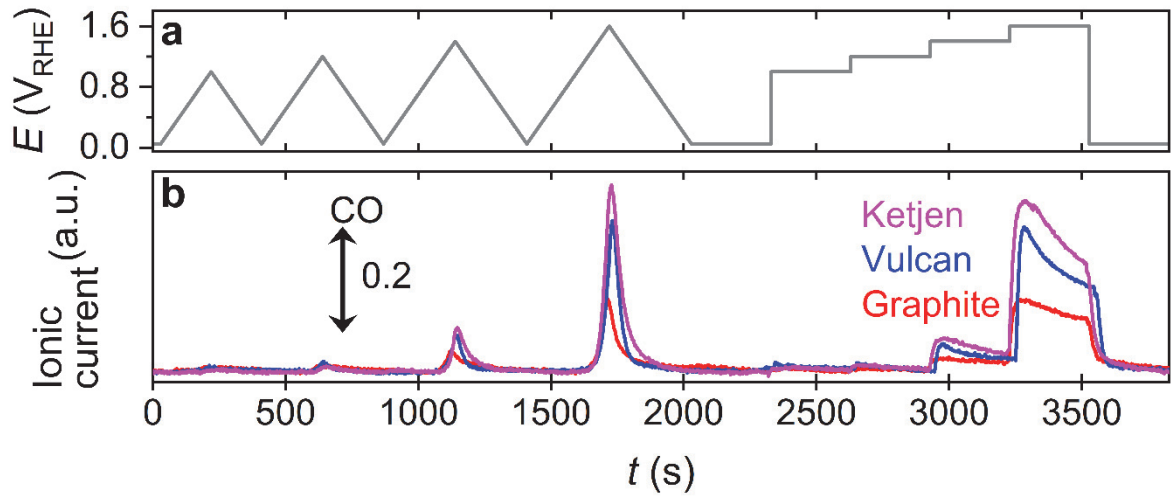

Figure S14. Comparison of the ionic current signals of CO for Ketjen, Vulcan, and Graphite substrates measured in an Ar-saturated 0.1 M $HClO_4$ electrolyte: (a) the potential protocol and (b) ionic current signal of CO.

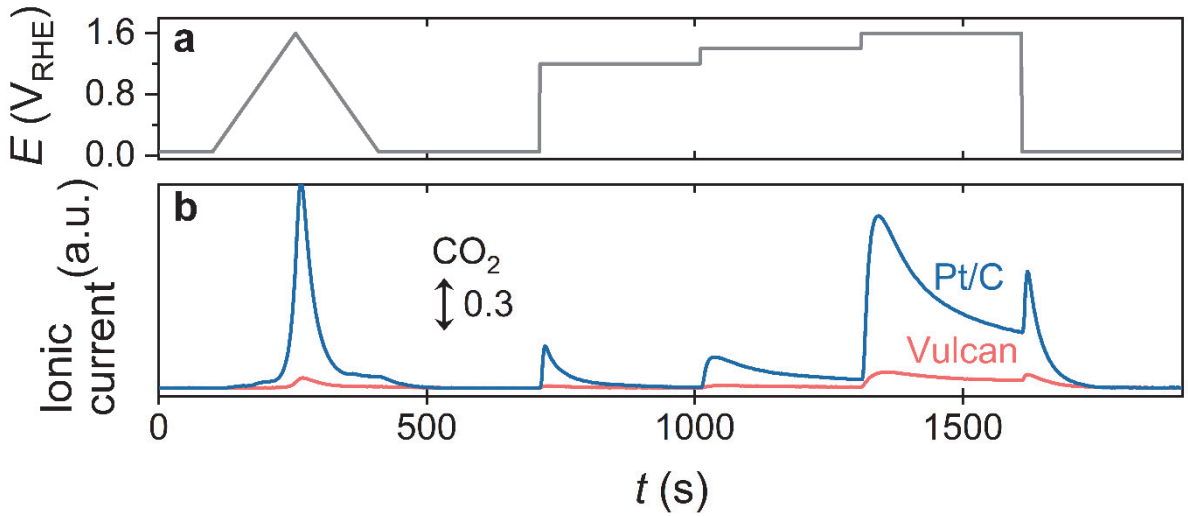

Figure S15. Online DEMS analysis of 5% Pt/C with the CO_2 tracer. (a) Potential protocol consisting of one CV from 0.05 to 1.6 V_{RHE} and three CAs at 1.2, 1.4, and 1.6 V_{RHE}. (b) The DEMS signals of CO_2 monitored in an Ar-saturated 0.1 M $HClO_4$ electrolyte. The result obtained with Vulcan is shown for comparison.

Note: For Pt/C, a small amount of CO_2 evolution, which was hardly observed with the Pt-free carbon substrate, was observed even at a relatively low potential of >0.6 V_{RHE}. Willsau *et al.* reported that this carbon corrosion at the low potential region is attributed to the Pt-catalyzed oxidation of surface functional groups (*e.g.*, carbonyl group).[1] At the potential of >0.8 V_{RHE}, considerable carbon corrosion occurred on the Pt/C as that on Pt-free carbon substrates, but quantitatively stronger corrosion of carbon was determined for the Pt/C. These results indicate that Pt effectively catalyzes carbon corrosion, as already known by several previous studies on CO_2 tracers in acidic electrolytes.[2, 3]

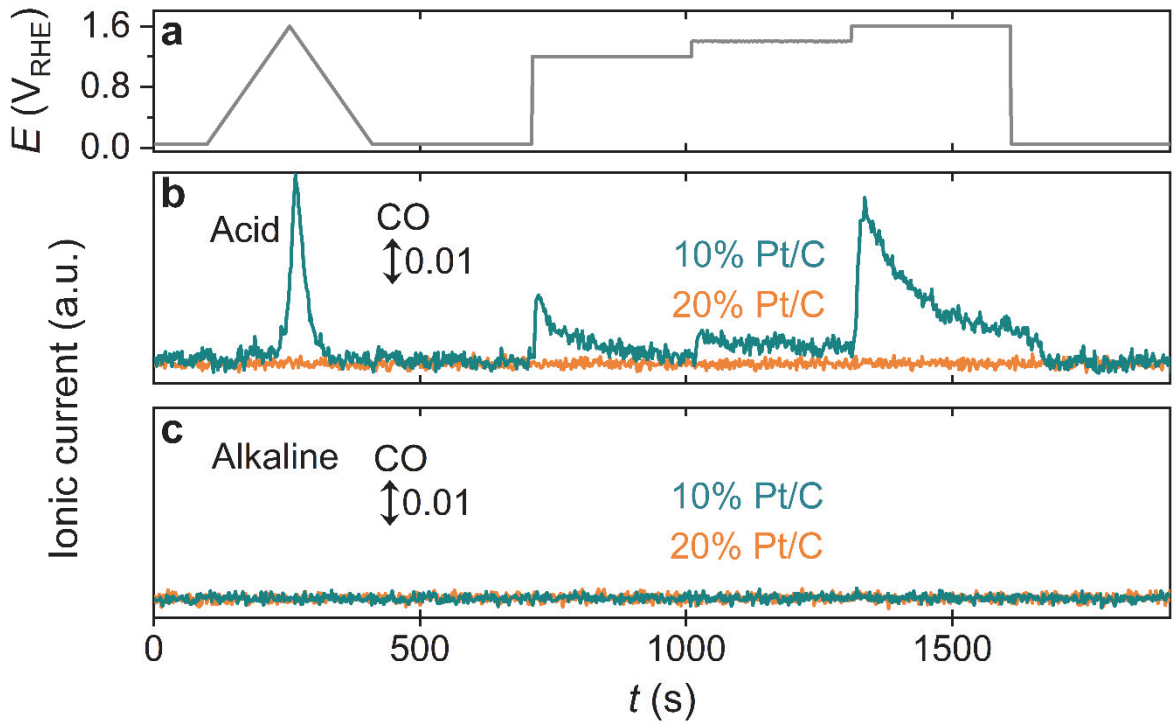

Figure S16. Online DEMS analysis of 10 and 20% Pt/C with the CO tracer. (a) Potential protocol consisting of one CV from 0.05 to 1.6 V_{RHE} and three CAs at 1.2, 1.4, and 1.6 V_{RHE}. (b and c) The DEMS signals of CO monitored in an Ar-saturated 0.1 M $HClO_4$ (b) and KOH (c) electrolytes.

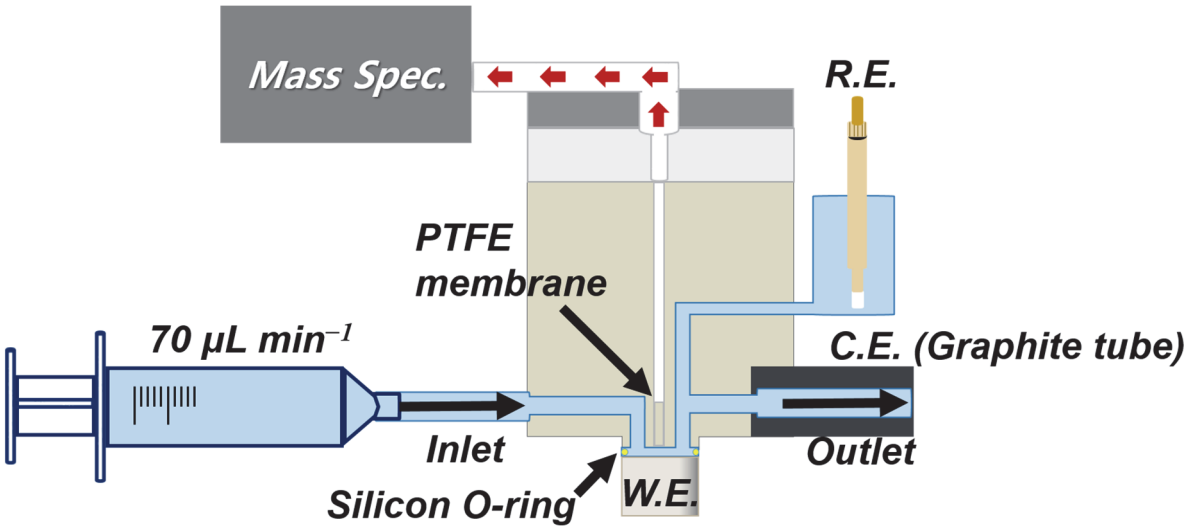

Figure S17. A schematic image of the online EFC–DEMS configuration.

Note: The electrolyte (Ar-saturated 0.1 M $HClO_4$ or KOH) continuously flowed into the EFC using the syringe pump (TYD01-01, LEADFLUID) at a flow rate of 70 μL min^{-1}, thus minimizing the disturbance of the mass signals induced by the accumulation of reaction products and bubble formation (*e.g.*, CO_2 and CO). Reference and graphite tube counter electrodes were mounted at the electrolyte outlet of the EFC to prevent contamination of the working electrode and interference with DEMS signals, which possibly originated from the leakage of the reference electrodes and CO/CO_2 formation from the counter electrode. The EFC with a U-shaped channel had an opening diameter of 1 cm at the bottom of the cell, where it made contact with the working electrode (commercial glassy carbon disk electrode with 3 mm diameter, A-011169, Bio-Logic). A tip with a porous Teflon membrane was located approximately 100 μm above the sample to allow the direct introduction of volatile species into the mass spectrometer. The positioning was monitored and adjusted using a digital microscope (MSP-8000, DIGIBIRD).

Reference

1. J. Willsau and J. Heitbaum, *J. Electroanal. Chem.*, 1984, **161**, 93-101.
2. S. Maass, F. Finsterwalder, G. Frank, R. Hartmann and C. Merten, *J. Power Sources*, 2008, **176**, 444-451.
3. L. Castanheira, W. O. Silva, F. H. B. Lima, A. Crisci, L. Dubau and F. Maillard, *ACS Catal.*, 2015, **5**, 2184-2194.